

pubs.acs.org/JACS Article

Synthesis of Allenes by Hydroalkylation of 1,3-Enynes with Ketones Enabled by Cooperative Catalysis

Maxwell Eaton, Yuping Dai, Ziyong Wang, Bo Li, Walid Lamine, Karinne Miqueu,* and Shih-Yuan Liu*



Cite This: J. Am. Chem. Soc. 2023, 145, 21638-21645



ACCESS I

III Metrics & More

Article Recommendations

Supporting Information

ABSTRACT: A method for the synthesis of allenes by the addition of ketones to 1,3-enynes by cooperative Pd(0)Senphos/ $B(C_6F_5)_3/NR_3$ catalysis is described. A wide range of aryl- and aliphatic ketones undergo addition to various 1,3-enynes in high yields at room temperature. Mechanistic investigations revealed a rate-determining outer-sphere proton transfer mechanism, which was corroborated by DFT calculations.

INTRODUCTION

Allenes are common structural motifs in natural products, bioactive small molecules, and materials.¹ They are also versatile synthetic intermediates, and many powerful transformations of allenes have been developed in recent years.^{2–4} Therefore, methods for efficient allene synthesis have been sought after by researchers.⁵ Of the many elegant catalytic methods, palladium-catalyzed hydrofunctionalization of conjugated enynes has emerged as an atom-economical approach for the preparation of allenes.⁶ In particular, hydroalkylation of 1,3-enynes allows allene synthesis with concomitant C–C bond formation, and some enantioselective processes have recently been developed (Scheme 1a).⁷ However, current methods require highly stabilized carbon pronucleophiles bearing multiple electron-withdrawing groups or activated 1,3-enynes.

In general, intermolecular hydroalkylation of unsaturated hydrocarbons using relatively unactivated pronucleophiles, specifically ketones, is rare, with only a few reported examples. 8-10 Since Dong's seminal work describing rhodium-catalyzed hydroalkylation of unactivated olefins with ketones (Scheme 1b), 11 the hydroalkylation of dienes (Scheme 1c)¹² and alkynes (Scheme 1d)¹³ with ketones has also been developed. 14 However, due to the lower reactivity of a ketone's α -C-H bond compared to more activated methylene compounds (e.g., malonates), 15 these methods typically require elevated temperatures. Additionally, there is no reported protocol for the hydroalkylation of 1,3-enynes with simple ketones. Given the synthetic utility of the ketone functionality and its prevalence in natural products and bioactive compounds, 16 a method allowing the mild, direct allenylation of ketones would represent a useful approach for building molecular complexity and late-stage functionalization of ketone-containing molecules. Here, we describe the development of a mild and general method for the hydroalkylation of 1,3-enynes with ketones via Pd(0)Senphos/

Scheme 1. Metal-Catalyzed Intermolecular Hydroalkylation

a) Pd(0)-catalyzed hydroalkylation of 1,3-enynes with "activated" pronucleophiles

b) Rh(I)-catalyzed directed hydroalkylation of olefins with ketones

$$\begin{array}{c|c} O \\ R^1 \\ R^2 \\ \bullet \text{ less "activated"} \end{array} \qquad \begin{array}{c} \text{cat. [Rh]/L} \\ \text{cat. HNR} \sim \text{DG} \\ \text{cat. TsOH} \\ \text{toluene,} \\ \bullet \text{ common motif} \end{array} \qquad \begin{array}{c|c} R \\ R^2 \\ \bullet R^1 \\ \bullet R^2 \\ \bullet R^1 \\ \bullet R^2 \\ \bullet$$

c) Ni(0)-catalyzed hydroalkylation of 1,3-dienes with ketones

d) Pd(0)/Proline-catalyzed hydroalkylation of alkynes with ketones

e) This work: Hydroalkylation of 1,3-enynes with ketones

Received: July 28, 2023

Published: September 22, 2023





 $B(C_6F_5)_3$ /amine base cooperative catalysis. The protocol is atom economical (no stoichiometric additives) and tolerates a wide range of both enynes and ketones to afford allenes in high yields after only a few hours at room temperature in most cases (Scheme 1e).

RESULTS AND DISCUSSION

Recently our group has reported a series of borofunctionalizations of 1,3-enynes using palladium(0) supported by our Senphos ligands.¹⁷ These reactions are hypothesized to proceed through an outer-sphere oxidative addition pathway involving activation of a palladium(0)-bound enyne by an electrophilic boron reagent. 18 We also recently developed a hydroalkynylation reaction utilizing cooperative Pd(0)-Senphos/B(C₆F₅)₃/NR₃ catalysis. ¹⁹ We therefore envisioned that a dual catalytic system of palladium(0) and B(C₆F₅)₃/NR₃ could activate both the 1,3-enyne and the ketone simultaneously to promote addition of the ketone α -C–H across the enyne.²⁰

To evaluate the feasibility of the proposed transformation, acetophenone 1a and envne 2a were used as model substrates (Table 1). In the presence of 2.5 mol % (1,5-cyclooctadiene)bis(trimethylsilylmethyl)palladium(II), [(COD)Pd-(CH₂TMS)₂], 3.0 mol % L11, 10 mol % tris(pentafluorophenyl)borane $[B(C_6F_5)_3]$, and 10 mol % 1,2,2,6,6pentamethylpiperidine (PMP) in toluene, the desired allene product 3a was formed in 92% yield after 1 h at room

Table 1. Survey of Ligands^a

Entry	Ligand	Yield (%) ^b
1	L1	0
2	L2	0
3	L3	0
4	L4	0
5	L5	0
6	L6	<5
7	L7	<5
8	L8	47
9	L9	78
10	L10	48
11	L11	92

^aSee Supporting Information for detailed procedures. ^bYields were determined by ¹H NMR analysis using 1,3,5-trimethoxybenzene as an internal standard.

temperature (entry 11). The use of bisphosphines (L1-L4) resulted in no observed product formation, and trialkyl phosphines (L5-L6) gave only a trace or no product. The commercially available monophosphine MOP (L7) also afforded a trace product. Modifications to the Senphos ligand's lower aryl fragment (L8-L9) led to lower product yields. Use of the structurally related, commercially available MePhos (L10) resulted in only moderate yield of the product, underscoring the importance of the unique electronic structure conferred by the 1,4-azaborine ring.²¹ No product formation was observed with any of the other Lewis acids tested, and other solvents examined resulted in diminished yields (see the Supporting Information, Table S1).

With the optimized conditions in hand, we next explored the substrate scope with respect to the ketone (Table 2). A wide

Table 2. Reaction Scope of Ketones^{a,b}

^aYields of isolated products are reported as an average of two trials. ^bSee Supporting Information for details. ^c48 h reaction time. ^a6:1 CH₂Cl₂:toluene used as solvent.

range of substituted acetophenones (aryl ethers, amines, and halides) are tolerated under the reaction conditions (entries 3a-3g). Larger naphthyl ketones (entry 3h), secondary aryl ketones (entry 3i), ortho-substituted aryl ketones (entry 3j), and heteroaryl ketones (entries 3k-3m) also react efficiently. Acyclic (entry 3n) and cyclic aliphatic ketones (entries 3o-3q) are also accepted. Notably, an enone (entry 3r) also serves as a suitable substrate, albeit furnishing the product with a diminished yield. The observed diastereomeric ratios (d.r.) with secondary ketone substrates are generally low. On the other hand, with unsymmetrical aliphatic ketones (entries 1s

and 1t), the observed regioneric ratio (r.r.) is moderate to excellent with the more substituted α -C-H undergoing addition to the enyne preferentially. This is likely due to preferential formation of the thermodynamically more stable enolate under the reaction conditions. More complex biologically active ketones (e.g., entry 1u) also undergo efficient conversion to the corresponding allenes, demonstrating the potential of the method for late-stage functionalization.

We next investigated the scope with respect to the 1,3enyne. As can be seen from Table 3, a range of para- and ortho-

Table 3. Reaction Scope of 1,3-Enynes^{a,b}

^aYields of isolated products are reported as an average of two trials. ^bSee Supporting Information for details. ^cReaction carried out at 45 °C for 18 h. ^dReaction carried out at 50 °C for 48 h.

substituted aryl enynes are well-tolerated (entries 4a-4d). Alkyl enynes (e.g., entry 4f) are also suitable substrates along with 1,3-disubstituted enynes (entries 4e and 4g). A 1,4disubstituted enyne (entry 4h) and a 1,2,4-trisubstituted enyne (entry 4i) also furnish the corresponding coupling products, although in only moderate yield. Various acid-sensitive functional groups, such as silvl ethers, esters, protected amines, and alkyl halides, are compatible with the reaction protocol (entries 4i-4m).

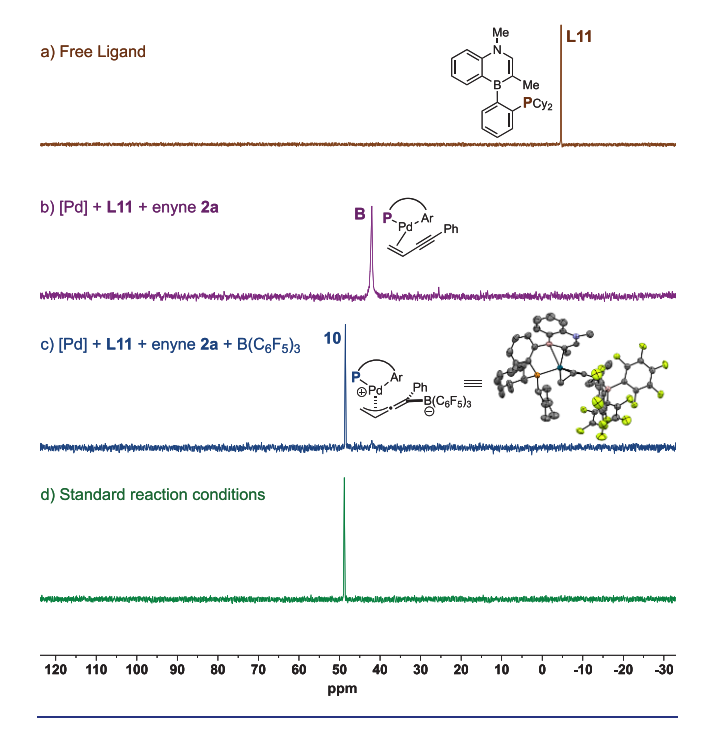
The process is also amenable to gram-scale procedure, with compound 3n being produced on 7.5 mmol scale in 80% yield using 1.0 mol % of the palladium catalyst (Scheme 2). Compound 3n serves as a useful intermediate for a variety of derivatizations. TiCl₄-mediated methylation²² affords tertiary alcohol 5, which can further undergo Au-catalyzed intramolecular hydroalkoxylation to yield furan derivative **6** in high yield and diastereoselectivity. ²³ Cu-mediated intramolecular reductive coupling produces cyclohexenol 7 in good yield and excellent diastereoselectivity.²⁴ Cu-catalyzed borylation²⁵ affords cyclic trisubstituted alkenyl-Bpin 8, which can then

Scheme 2. Gram-Scale Synthesis and Product Derivatization

undergo Suzuki-Miyaura coupling to furnish densely functionalized cyclohexenol 9 in high yield.

To elucidate the reaction mechanism, we carried out a series of mechanistic studies. First, we sought to identify the ³¹P NMR signals of some likely catalytic intermediates. Free ligand L11 exhibits a signal at -2.8 ppm (Scheme 3a). A 1:1 mixture

Scheme 3. Pd Catalyst Resting State Determination by ³¹P **NMR**



of the palladium precursor (COD)Pd(CH2TMS)2, L11, and excess enyne 2a in toluene results in a broad resonance at 42.4 ppm, which we assign as the enyne-bound palladium complex B (Scheme 3b). Outer-sphere oxidative addition adduct 10 was independently isolated and fully characterized by NMR spectroscopy and X-ray crystallography (see Supporting Information for details) and features a sharp signal at 48.8 ppm (Scheme 3c). When the catalytic reaction under standard

conditions was analyzed by ³¹P NMR, only a single resonance at 48.6 ppm was observed (Scheme 3d), consistent with complex 10 being the resting state of the Pd catalyst.

We next evaluated the resting state(s) of the boron catalyst by ¹¹B NMR. A combination of the palladium precursor, L11, $B(C_6F_5)_3$, and excess enyne produces a sharp resonance at -11.0 ppm, originating from the tetracoordinate boron of complex 10 (Scheme 4a). The free $B(C_6F_5)_3$ appears as a

Scheme 4. $B(C_6F_5)_3$ Catalyst Resting State Determination by 11B NMR

a) [Pd] + L11 + enyne 2a + B(C₆F₅)₃
$$B(C_9F_5)_3$$
b) [Pd] + L11 + enyne 2a + B(C₆F₅)₃ + ketone 1a

c) [Pd] + L11 + enyne 2a + B(C₆F₅)₃ + ketone 1a + PMP (Standard conditions)

1a-NH (Standard conditions)

broad signal at 60 ppm. Addition of excess ketone results in an additional broad signal at 2.3 ppm, consistent with the acetophenone-B(C_6F_5)₃ Lewis pair 1a-BCF (Scheme 4b).²⁶ Upon addition of PMP base (simulating the standard reaction conditions), the signal at 2.3 ppm shifts upfield to -3.0 ppm, which is consistent with an anionic, tetracoordinate boron species.²⁷ Thus, we assign the signal at -3.0 ppm as the ammonium O-boron enolate 1a-NH.

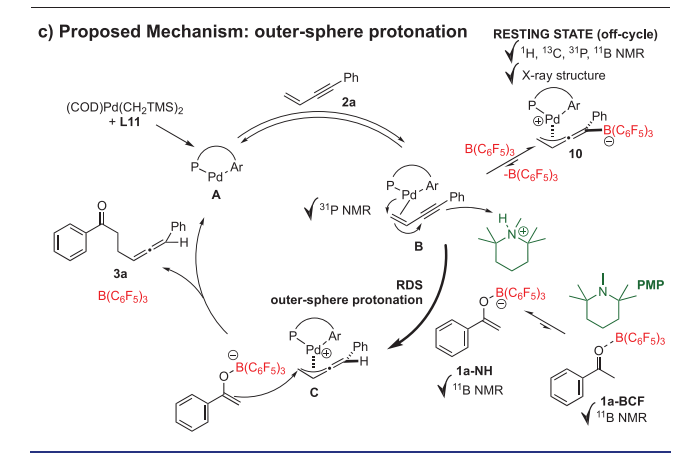
Independent kinetic isotope effect (KIE) measurements were carried out using initial rate kinetics to probe the nature of the rate-determining step. A relatively large primary KIE of $k_{\rm H}/k_{\rm D}$ = 4.5 \pm 0.2 was measured for the reaction of 1a vs 1a-d₈ in toluene-d₈ (Scheme 5a), consistent with the ratedetermining transition state involving X-H bond cleavage. Additionally, the kinetic order of each reactant and catalyst was experimentally determined via reaction progress kinetic analysis (RPKA)²⁸ (see Supporting Information for details) using ketone 1a and 1,3-enyne 2a as model substrates. Different-excess experiments revealed a zero-order dependence of the reaction rate on both substrates (1a and 2a), and a first order dependence on the total palladium catalyst concentration [Pd/L]₀. The reaction orders with respect to the total concentrations of Lewis acid catalyst $[B(C_6F_5)_3]_0$, and amine base catalyst [PMP]₀ depend on their relative catalyst loadings. When the Lewis acid is in excess of the base, the reaction is inverse first order in $[B(C_6F_5)_3]_0$, and first order in $[PMP]_0$. When the base is in excess of the Lewis acid, the reaction is zero order in $[B(C_6F_5)_3]_0$ and zero order in $[PMP]_0$ (Scheme

A proposed catalytic cycle is illustrated in Scheme 5c. In the presence of L11, the palladium precursor undergoes reductive elimination and loss of its COD ligand to form the Pd(0)/ Scheme 5. Kinetic Isotope Effect, Rate Law, and Proposed Mechanism

a) Independent KIE Measurement

b) Experimentally Determined Rate Law

Rate = $d[3a]/dt = k_{obs}[1a]^0 [2a]^0 [Pd/L]_0^1 [B(C_6F_5)_3]_0^x [PMP]_0^y$ When $[B(C_6F_5)_3]_0 > [PMP]_0$, $x \approx -1$, $y \approx 1$ When $[B(C_6F_5)_3]_0 < [PMP]_0$, $x \approx 0$, $y \approx 0$



Senphos complex A, which binds enyne 2a to form B. Intermediate B exists in equilibrium with off-cycle complex 10, which we have identified as the resting state of the Pd catalyst. For productive catalysis to occur, 10 must dissociate $B(C_6F_5)_3$ to reform B, which undergoes a rate-determining outer-sphere protonation 7a,29,30 of the palladium-bound enyne with ammonium enolate 1a-NH to generate C. Intermediate C is then attacked by the boron enolate to generate product 3a and regenerate palladium catalyst A and $B(C_6F_5)_3$ catalyst.

This cooperative catalytic system can be broken down into two catalytic cycles: (1) Pd-based cycle acting on the envne substrate (2a) and (2) B(C₆F₅)₃/PMP-based "cycle" acting on the ketone substrate (1a). Each catalyst is saturated with its respective substrate (i.e., Pd catalyst is completely saturated with the 1,3-enyne substrate and the $B(C_6F_5)_3/PMP$ catalysts are saturated with the ketone substrate to a large extent, see Schemes 3 and 4) in both the resting state and the rate-limiting transition state, consistent with the observed zero-order kinetics with respect to both ketone (1a) and enyne (2a) substrates. The rate-determining step involves a proton transfer that is consistent with the observed primary kinetic isotope effect. When excess $B(C_6F_5)_3$ is present relative to the Pd/ Senphos catalyst (standard conditions), the catalysis is inhibited due to formation of the catalytically inactive 10, leading to inverse-first order contribution of B(C₆F₅)₃ to the rate-expression for product formation for the Pd-based cycle. A simplified approximated product-forming rate expression based on limiting parameters (e.g., equilibria from experimental data)

$$d[\mathbf{3a}]/dt \approx k_{\text{obs}}[\mathbf{2a}]^{0} [Pd/L]_{0}^{1} [B(C_{6}F_{5})_{3}]_{0}^{-1} [\mathbf{1a}-\mathbf{NH}]^{1}$$
 (1)

The second B(C₆F₅)₃/PMP cycle contributes to the [1a-NH]1 term of the "main" rate expression (eq 1). In this $B(C_6F_5)_3$ /PMP cycle, when one catalyst is in excess of the

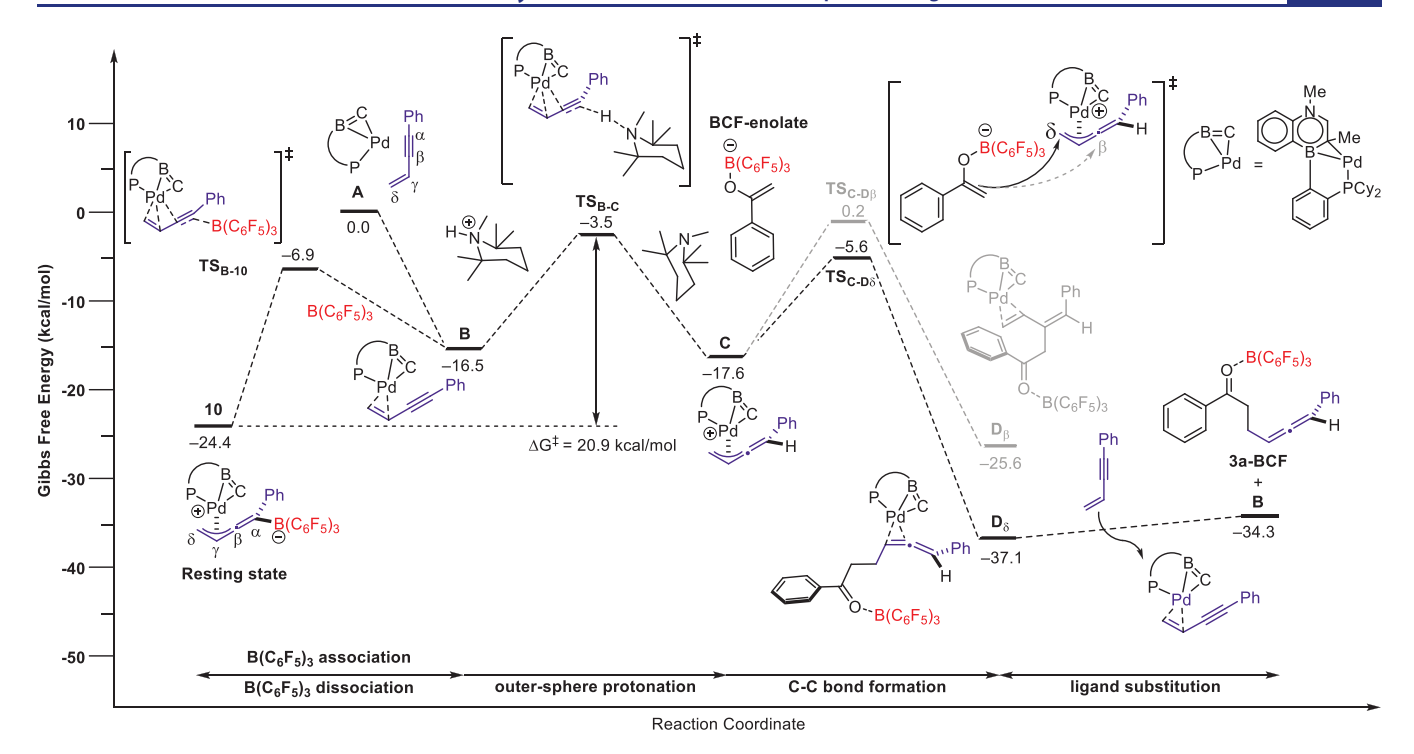


Figure 1. Energy profile (ΔG in kcal/mol) computed at the SMD(toluene)-ωB97X-D/SDD+f(Pd), 6-31G+**(other atoms)//SMD(toluene)ωB97X-D/SDD+f(Pd), 6-31G**(other atoms) level of theory for the proposed outer-sphere protonation mechanism where the protonated amine base PMP-H⁺ oxidatively activates the Pd-enyne complex B. For the energy profiles of alternative mechanisms, see the Supporting Information.

other, the catalyst in excess will also experience "saturation" with respect to the limiting catalyst and no longer "contributes" (i.e., zero-order kinetics) to the formation of the ammonium enolate [1a-NH].³¹ Thus, when $[B(C_6F_5)_3]_0 >$ $[PMP]_0$, it follows that $[1a-NH] \approx [PMP]_0^{-1} [1a]^0$, resulting in the overall expression:

$$d[\mathbf{3a}]/dt \approx k_{\text{obs}}[\mathbf{1a}]^0[\mathbf{2a}]^0[\text{Pd/L}]_0^{\ 1}[\text{B}(\text{C}_6\text{F}_5)_3]_0^{\ -1}[\text{PMP}]_0^{\ 1}$$
(2

On the other hand, when $[B(C_6F_5)_3]_0 < [PMP]_0$, it follows that $[\textbf{1a-NH}] \approx [B(C_6F_5)_3]_0^1 \ [\textbf{1a}]^0$, resulting in the overall expression:

$$d[\mathbf{3a}]/dt \approx k_{\text{obs}}[\mathbf{1a}]^{0}[\mathbf{2a}]^{0}[\text{Pd/L}]_{0}^{1}[\text{B(C}_{6}F_{5})_{3}]_{0}^{0}[\text{PMP}]_{0}^{0}$$
(3)

The above simplified kinetic model (eqs 1-3) is consistent with our observed cocatalyst concentration dependent rate laws as shown in Scheme 5b. Thus, our proposed mechanism, including the assignment of the resting states and ratedetermining step, is consistent with all the experimentally observed spectroscopic and kinetic data.

Density functional theory (DFT) calculations were carried out at SMD³²(toluene)- ω B97X-D³³/SDD+f(Pd), ³⁴ 6- $31+G^{**}(other atoms)//SMD(toluene)-\omega B97X-D/SDD+f-$ (Pd),6-31G**(other atoms) level of theory (see Supporting Information for computational details) to additionally probe the mechanism of the Pd(0)Senphos/B(C₆F₅)₃/PMP-catalyzed hydroalkylation of enynes. We computationally considered three mechanistic scenarios (see Supporting Information, Scheme S1): (1) outer-sphere protonation pathway (i.e., mechanism illustrated in Scheme 5c), (2) protodeboronation pathway where the resting state species 10 is protonated with PMP-H⁺ with concomitant release of $B(C_6F_5)_3$ to form C_7 (3) Pd(II)—H pathway where the PMP-H⁺ oxidatively adds to

Pd(0) species A to form a Pd(II)-H intermediate that then subsequently undergoes β -migratory insertion ^{14b,36} into the 1,3-enyne to furnish the *syn*-diastereomer of the π -allyl intermediate C (i.e., H and Pd are oriented syn to each other).

DFT calculations predict that Pd(0)/Senphos complex A coordinates to the C=C double bond of the 1,3-enyne to form the π -complex **B** in an exergonic fashion (Figure 1). We considered two possible isomers for the π -complex (Figures S1 and S2): B (alkene is cis to the P atom of the Senphos ligand) and B' (alkene is *trans* to the P atom of the Senphos ligand). Structure B has been found to be more stable (by >1.3 kcal/ mol) than B' throughout the reaction coordinate. This predicted orientational preference is consistent with the obtained crystal structure for resting state complex 10 (Scheme 3c). The π -complex **B** kinetically prefers $(\Delta G^{\ddagger}_{B-10} = 9.6 \text{ kcal/}$ mol) to undergo an outer-sphere oxidative addition with $B(C_6F_5)_3$ to furnish complex 10 via an early transition state TS_{B-10} (B···C_a: 2.493 Å and ΣB_{λ} : 352.45°). Intermediate 10 is the computationally predicted resting state of the Pd catalyst, which agrees with the experimentally observed data (spectroscopic evidence, see Scheme 3; kinetic evidence, see Scheme 5b). The optimized structure of the Pd- π -allyl intermediate 10 $(Pd-C_{\beta}, Pd-C_{\gamma}, Pd-C_{\delta}: 2.346, 2.182, and 2.088 Å,$ respectively; B-C_a: 1.702 Å) reproduces the obtained X-ray crystallographic data.

Complex 10 can readily dissociate $B(C_6F_5)_3$ to reform π complex **B** ($\Delta G^{\ddagger}_{10 \to TSB-10} = 17.5 \text{ kcal/mol}$), which can then be protonated by PMP-H⁺ (i.e., the proton source component of the ion pair 1a-NH, N-H: 1.025 Å) with a barrier $\Delta G^{\ddagger}_{B-C}$ = 13.0 kcal/mol to form the alkylidene- π -allylpalladium intermediate C (C_α -H: 1.091 Å; $Pd-C_\beta$, $Pd-C_\gamma$, $Pd-C_\delta$: 2.144, 2.154, and 2.166 Å, respectively). In the transition state TS_{B-C} , the C_{α} ···H and N···H bonds are 1.425 and 1.293 Å, respectively, and the $\angle C_\alpha HN = 175^\circ$ bond angle is almost

linear. In contrast to the structure of intermediate C, the allyl moiety in TS_{B-C} is nonsymmetrically coordinated to Pd (Pd- C_{β} , Pd $-C_{\gamma}$, Pd $-C_{\delta}$: 2.527, 2.201, and 2.076 Å, respectively), which is consistent with the Pd mostly maintaining an η^2 coordination with the alkene. From C, a nucleophilic attack by the BCF-enolate (i.e., the boron enolate component of the ion pair 1a-NH) occurs with a $\Delta \Delta G^{\ddagger} = 5.8$ kcal/mol kinetic preference toward the C_{δ} position over the C_{β} position to generate allene product D_{δ} . Product 3a is then released to start a new catalytic cycle. The nucleophilic attack is relatively facile, with a predicted barrier of $\Delta G^{\ddagger}_{C \to TSC \cdot D\delta} = 12.0 \text{ kcal/mol}$. The calculated overall rate-limiting barrier $\Delta G^{\ddagger}_{10 \rightarrow \text{TSB-C}}$ of 20.9 kcal/mol, the predicted $k_{\rm H}/k_{\rm D}({\rm DFT})=6.1$, and the off-cycle resting state 10 for the proposed outer-sphere protonation pathway are consistent with experimental observations.

For mechanistic scenario (2): the protodeboronation pathway (see Supporting Information, Figure S3), DFT calculations show that the protodeboronation process occurs in 2 steps: (i) a proton transfer from PMP-H⁺ to C_{β} carbon of complex 10, which is followed by (ii) a [1,2]-H (hydride) shift from C_{β} to C_{α} position with concomitant release of $B(C_6F_5)_3$ to furnish C. The predicted rate-limiting barrier for this pathway is $\Delta G^{\ddagger} = 48.1$ kcal/mol, which is inconsistent with a room-temperature reaction.

For mechanistic scenario (3): the Pd(II)-H pathway (see Figure S4), we computed the energy profile involving direct protonation of Pd(0)/Senphos complex A by PMP-H⁺ followed by Pd-H β -migratory insertion into the triple bond of the 1,3-enyne. The direct protonation of Pd complex A is predicted to be energetically costly, with a rate-limiting barrier of ΔG^{\ddagger} = 52.7 kcal/mol (from the resting state 10), which is also inconsistent with a room-temperature reaction.

CONCLUSIONS

We developed a mild, general method for hydroalkylation of 1,3-enynes with ketones to generate allenes. A broad range of aryl and alkyl ketones could be coupled with 1,3-enynes to provide synthetically useful β -allenyl ketones in a high yield. To the best of our knowledge, this work represents a rare example of room-temperature metal-catalyzed addition of a ketone α -C-H bond to an unsaturated hydrocarbon. Mechanistic studies reveal that the outer-sphere oxidative addition adduct 10 is an off-cycle resting state during catalysis. The rate-determining step involves a proton transfer with an accessible activation barrier computed at 20.9 kcal/mol. DFT calculations are in agreement with the experimental kinetics and spectroscopic observations. The body of our mechanistic investigations points toward a multifaceted and intricate behavior underlying the Pd/Senphos-catalyzed activation of 1,3-enynes, and we hope this work will serve as inspiration for the further development of mild and general catalytic systems which activate $C(sp_3)$ –H bonds for addition to C–C π -bonds.

ASSOCIATED CONTENT

Supporting Information

The Supporting Information is available free of charge at https://pubs.acs.org/doi/10.1021/jacs.3c08151.

Experimental procedures, compound characterization data, computational and crystallographic information (PDF)

Optimized Cartesian coordinates (XYZ)

Accession Codes

CCDC 2278579 and 2278580 contain the supplementary crystallographic data for this paper. These data can be obtained free of charge via www.ccdc.cam.ac.uk/data_request/cif, or by emailing data request@ccdc.cam.ac.uk, or by contacting The Cambridge Crystallographic Data Centre, 12 Union Road, Cambridge CB2 1EZ, UK; fax: + 44 1223 336033.

AUTHOR INFORMATION

Corresponding Authors

Shih-Yuan Liu – Department of Chemistry, Boston College, Chestnut Hill, Massachusetts 02467-3860, United States; E2S UPPA/CNRS, Institut des Sciences Analytiques et de Physico-Chimie pour l'Environnement et les Matériaux IPREM UMR 5254, Université de Pau et des Pays de l'Adour, 64053 Pau Cedex 09, France; o orcid.org/0000-0003-3148-9147; Email: shihyuan.liu@bc.edu

Karinne Miqueu – E2S UPPA/CNRS, Institut des Sciences Analytiques et de Physico-Chimie pour l'Environnement et les Matériaux IPREM UMR 5254, Université de Pau et des Pays de l'Adour, 64053 Pau Cedex 09, France; o orcid.org/ 0000-0002-5960-1877; Email: karinne.miqueu@univpau.fr

Authors

Maxwell Eaton – Department of Chemistry, Boston College, Chestnut Hill, Massachusetts 02467-3860, United States Yuping Dai - E2S UPPA/CNRS, Institut des Sciences Analytiques et de Physico-Chimie pour l'Environnement et les

Matériaux IPREM UMR 5254, Université de Pau et des Pays de l'Adour, 64053 Pau Cedex 09, France Ziyong Wang – Department of Chemistry, Boston College,

Chestnut Hill, Massachusetts 02467-3860, United States; orcid.org/0000-0002-6585-8951

Bo Li – Department of Chemistry, Boston College, Chestnut Hill, Massachusetts 02467-3860, United States

Walid Lamine - E2S UPPA/CNRS, Institut des Sciences Analytiques et de Physico-Chimie pour l'Environnement et les Matériaux IPREM UMR 5254, Université de Pau et des Pays de l'Adour, 64053 Pau Cedex 09, France

Complete contact information is available at: https://pubs.acs.org/10.1021/jacs.3c08151

Author Contributions

M.E. performed the experimental synthetic and mechanistic work guided by S.-Y.L. Y.D. performed the computational work guided by K.M. Z.W. discovered the title reaction and performed preliminary reaction optimization. B.L. solved the X-ray structures. W.L. provided initial computational analysis. The manuscript was written through contributions of all authors. All authors have given approval to the final version of the manuscript.

Notes

The authors declare no competing financial interest.

ACKNOWLEDGMENTS

Research reported in this publication was supported by the National Institute of General Medical Sciences of the National Institutes of Health (NIGMS) under Award Number R01GM136920, the Excellence Initiative of Université de Pau et des Pays de l'Adour I-Site E2S UPPA, and by Boston College start-up funds. We also acknowledge the NIH-S10

(award: 1S10OD026910-01A1) and the NSF-MRI (award: CHE-2117246) for the support of Boston College's NMR facilities. Part of this work was granted access to the HPC resources of [CCRT/CINES/IDRIS] under the allocation 2022 [AD010800045R1] made by GENCI (Grand Equipement National de Calcul Intensif) and Mésocentre de Calcul Intensif Aquitain (MCIA). The "Direction du Numérique" of UPPA is also acknowledged for supporting computational facilities. Z.W. was supported as a LaMattina Graduate Fellow in Chemical Synthesis. Y.D. and W.L. were funded as a Ph.D. and postdoctoral fellow, respectively, by I-Site E2S-UPPA.

DEDICATION

This work is dedicated to Prof. Gregory C. Fu on the occasion of his 60th birthday.

REFERENCES

- (1) For an overview, see: (a) Hoffmann-Röder, A.; Krause, N. Synthesis and Properties of Allenic Natural Products and Pharmaceuticals. Angew. Chem., Int. Ed. 2004, 43, 1196-1216. (b) Rivera-Fuentes, P.; Diederich, F. Allenes in Molecular Materials. Angew. Chem., Int. Ed. 2012, 51, 2818-2828.
- (2) Ma, S. Some Typical Advances in the Synthetic Applications of Allenes. Chem. Rev. 2005, 105, 2829-2872.
- (3) Allen, A. D.; Tidwell, T. T. Ketenes and Other Cumulenes as Reactive Intermediates. Chem. Rev. 2013, 113, 7287-7342.
- (4) Yu, S.; Ma, S. Allenes in Catalytic Asymmetric Synthesis and Natural Product Syntheses. Angew. Chem., Int. Ed. 2012, 51, 3074-3112.
- (5) For an overview, see: (a) Yu, S.; Ma, S. How easy are the syntheses of allenes? Chem. Commun. 2011, 47, 5384-5418. (b) Neff, R. K.; Frantz, D. E. Recent advances in the catalytic syntheses of allenes: a critical assessment. ACS Catal. 2014, 4, 519-528.
- (6) For hydrofunctionalization of enynes, see: (a) Yamamoto, Y.; Radhakrishnan, U. Palladium catalysed pronucleophile addition to unactivated carbon-carbon multiple bonds. Chem. Soc. Rev. 1999, 28, 199-207. (b) Salter, M. M.; Gevorgyan, V.; Saito, S.; Yamamoto, Y. Synthesis of Allenes via Palladium Catalysed Addition of Certain Activated Methynes to Conjugated Enynes. Chem. Commun. 1996, 32, 17-18. (c) Radhakrishnan, U.; Al-Masum, M.; Yamamoto, Y. Palladium Catalyzed Hydroamination of Conjugated Enynes. Tetrahedron Lett. 1998, 39, 1037-1040. (d) Fu, L.; Greßies, S.; Chen, P.; Liu, G. Recent Advances and Perspectives in Transition Metal-Catalyzed 1,4-Functionalizations of Unactivated 1,3-Enynes for the Synthesis of Allenes. Chin. J. Chem. 2020, 38, 91-100. (e) Dherbassy, Q.; Manna, S.; Talbot, F. J. T.; Prasitwatcharakorn, W.; Perry, G. J. P.; Procter, D. Copper-catalyzed functionalization of enynes. Chem. Sci. 2020, 11, 11380-11393. (f) Adamson, N. J.; Jeddi, H.; Malcolmson, S. J. Preparation of Chiral Allenes through Pd-Catalyzed Intermolecular Hydroamination of Conjugated Enynes: Enantioselective Synthesis Enabled by Catalyst Design. J. Am. Chem. Soc. 2019, 141, 8574-8583.
- (7) For enantioselective hydroalkylation of 1,3-enynes to prepare allenes, see: (a) Tsukamoto, H.; Konno, T.; Ito, K.; Doi, T. Palladium(0)-Lithium Iodide Cocatalyzed Asymmetric Hydroalkylation of Conjugated Enynes with Pronucleophiles Leading to 1,3-Disubstituted Allenes. Org. Lett. 2019, 21, 6811-6814. (b) Yang, S.-Q.; Wang, Y.-F.; Zhao, W.-C.; Lin, G.-Q.; He, Z.-T. Stereodivergent Synthesis of Tertiary Fluoride-Tethered Allenes via Copper and Palladium Dual Catalysis. J. Am. Chem. Soc. 2021, 143, 7285-7291. (c) Qian, H.; Yu, X.; Zhang, J.; Sun, J. Organocatalytic enantioselective synthesis of 2,3-allenoates by intermolecular addition of nitroalkanes to activated enynes. J. Am. Chem. Soc. 2013, 135, 18020–18023. (d) Yao, Q.; Liao, Y.; Lin, L.; Lin, X.; Ji, J.; Liu, X.; Feng, X. Efficient Synthesis of Chiral Trisubstituted 1,2-Allenyl Ketones by Catalytic Asymmetric Conjugate Addition of Malonic Esters to Enynes. Angew. Chem., Int. Ed. 2016, 55, 1859-1863.

- (8) For intramolecular hydroalkylation of olefins with ketones, see: (a) Wang, X.; Pei, T.; Han, X.; Widenhoefer, R. A. Palladiumcatalyzed intramolecular hydroalkylation of unactivated olefins with dialkyl ketones. Org. Lett. 2003, 5, 2699-2701. (b) Xiao, Y.-P.; Liu, X.-Y.; Che, C.-M. Efficient gold(I)-catalyzed direct intramolecular hydroalkylation of unactivated alkenes with α -ketones. Angew. Chem., Int. Ed. 2011, 50, 4937-4941.
- (9) For hydroalkylation of styrene derivatives with ketones, see: (a) Rodriguez, A. L.; Bunlaksananusorn, T.; Knochel, P. Potassium tert-butoxide catalyzed addition of carbonyl derivatives to styrenes. Org. Lett. 2000, 2, 3285-3287. (b) Majima, S.; Shimizu, Y.; Kanai, M. Cu(I)-catalyzed α -alkylation of ketones with styrene derivatives. Tetrahedron Lett. 2012, 53, 4381-4384. (c) Qiao, J.; Ci, R. N.; Gan, Q. C.; Huang, C.; Liu, Z.; Hu, H. L.; Ye, C.; Chen, B.; Tung, C. H.; Wu, L. Z. Amine-Free, Directing-Group-Free and Redox-Neutral alpha-Alkylation of Saturated Cyclic Ketones. Angew. Chem., Int. Ed. 2023, 62, No. e202305679.
- (10) For hydroalkylation reactions with aldehydes via SOMO activation, see: (a) Comito, R. J.; Finelli, F. G.; MacMillan, D. W. C. Enantioselective intramolecular aldehyde α -alkylation with simple olefins: Direct access to homo-ene products. J. Am. Chem. Soc. 2013, 135, 9358-9361. (b) Beeson, T. D.; Mastracchio, A.; Hong, J. B.; Ashton, K.; Macmillan, D. W. C. Enantioselective organocatalysis using SOMO activation. Science 2007, 316, 582-585.
- (11) (a) Mo, F.; Dong, G. Regioselective ketone α -alkylation with simple olefins via dual activation. Science 2014, 345, 68-72. (b) Xing, D.; Dong, G. Branched-Selective Intermolecular Ketone α -Alkylation with Unactivated Alkenes via an Enamide Directing Strategy. J. Am. Chem. Soc. 2017, 139, 13664-13667.
- (12) Cheng, L.; Li, M.-M.; Xiao, L.-J.; Xie, J.-H.; Zhou, Q.-L. Nickel(0)-Catalyzed Hydroalkylation of 1,3-Dienes with Simple Ketones. J. Am. Chem. Soc. 2018, 140, 11627-11630.
- (13) For amine/transition metal-cocatalyzed hydroalkylation using ketones and aldehydes, see: (a) Yang, C.; Zhang, K.; Wu, Z.; Yao, H.; Lin, A. Cooperative Palladium/Proline-Catalyzed Direct α -Allylic Alkylation of Ketones with Alkynes. Org. Lett. 2016, 18, 5332-5335. (b) Zhou, H.; Wang, Y.; Zhang, L.; Cai, M.; Luo, S. Enantioselective Terminal Addition to Allenes by Dual Chiral Primary Amine/ Palladium Catalysis. J. Am. Chem. Soc. 2017, 139, 3631-3634. (c) Cruz, F. A.; Dong, V. M. Stereodivergent Coupling of Aldehydes and Alkynes via Synergistic Catalysis Using Rh and Jacobsen's Amine. J. Am. Chem. Soc. 2017, 139, 1029-1032.
- (14) For intermolecular hydroalkylation of dienes and other unsaturated hydrocarbons with activated pronucleophiles, see: (a) Adamson, N. J.; Wilbur, K. C. E.; Malcolmson, S. J. Enantioselective Intermolecular Pd-Catalyzed Hydroalkylation of Acyclic 1,3-Dienes with Activated Pronucleophiles. J. Am. Chem. Soc. 2018, 140, 2761-2764. (b) Park, S.; Adamson, N. J.; Malcolmson, S. J. Bronsted acid and Pd-PHOX dual-catalysed enantioselective addition of activated C-pronucleophiles to internal dienes. Chem. Sci. 2019, 10, 5176-5182. (c) Adamson, N. J.; Park, S.; Zhou, P.; Nguyen, A. L.; Malcolmson, S. J. Enantioselective Construction of Quaternary Stereogenic Centers by the Addition of an Acyl Anion Equivalent to 1,3-Dienes. Org. Lett. 2020, 22, 2032-2037. (d) Leitner, A.; Larsen, J.; Steffens, C.; Hartwig, J. F. Palladium-Catalyzed Addition of Mono- and Dicarbonyl Compounds to Conjugated Dienes. J. Org. Chem. 2004, 69, 7552-7557. (e) Trost, B. M.; Simas, A. B. C.; Plietker, B.; Jäkel, C.; Xie, J. Enantioselective Palladium-Catalyzed Addition of 1,3-Dicarbonyl Compounds to an Allene Derivative. Chem. Eur. J. 2005, 11, 7075-7082. (f) Zhang, Q.; Yu, H.; Shen, L.; Tang, T.; Dong, D.; Chai, W.; Zi, W. Stereodivergent Coupling of 1,3-Dienes with Aldimine Esters Enabled by Synergistic Pd and Cu Catalysis. J. Am. Chem. Soc. 2019, 141, 14554-14559. (g) Shao, W.; Besnard, C.; Guénée, L.; Mazet, C. Ni-Catalyzed Regiodivergent and Stereoselective Hydroalkylation of Acyclic Branched Dienes with Unstabilized C(Sp3) Nucleophiles. J. Am. Chem. Soc. 2020, 142, 16486-16492. (h) Yang, H.; Xing, D. Palladium-Catalyzed Diastereo- and Enantioselective Allylic Alkylation of Oxazolones with 1,3-Dienes under Base-Free Conditions.

- Chem. Commun. 2020, 56, 3721–3724. (i) Zhang, Z.; Xiao, F.; Wu, H.-M.; Dong, X.-Q.; Wang, C.-J. Pd-Catalyzed Asymmetric Hydroalkylation of 1,3-Dienes: Access to Unnatural α-Amino Acid Derivatives Containing Vicinal Quaternary and Tertiary Stereogenic Centers. Org. Lett. 2020, 22, 569–574. (j) Wang, H.; Zhang, R.; Zhang, Q.; Zi, W. Synergistic Pd/Amine-Catalyzed Stereodivergent Hydroalkylation of 1,3-Dienes with Aldehydes: Reaction Development, Mechanism, and Stereochemical Origins. J. Am. Chem. Soc. 2021, 143, 10948–10962. (k) Chen, X.-X.; Luo, H.; Chen, Y.-W.; Liu, Y.; He, Z.-T. Enantioselective Palladium-Catalyzed Directed Migratory Allylation of Remote Dienes. Angew. Chem., Int. Ed. 2023, 62, No. e202307628. (l) Wang, X.; Miao, H.-Z.; Lin, G.-Q.; He, Z.-T. Ligand-Dictated Regiodivergent Allylic Functionalizations via Palladium-Catalyzed Remote Substitution. Angew. Chem., Int. Ed. 2023, 62, No. e202301556.
- (15) For addition of beta-ketoacids to alkynes, see: (a) Cruz, F. A.; Chen, Z.; Kurtoic, S. I.; Dong, V. M. Tandem Rh-Catalysis: Decarboxylative β -Keto Acid and Alkyne Cross-Coupling. *Chem. Commun.* **2016**, *52*, 5836–5839. (b) Li, C.; Grugel, C. P.; Breit, B. Rhodium-Catalyzed Chemo- and Regioselective Decarboxylative Addition of β -Ketoacids to Alkynes. *Chem. Commun.* **2016**, *52*, 5840–5843.
- (16) Foley, D. J.; Waldmann, H. Ketones as strategic building blocks for the synthesis of natural product-inspired compounds. *Chem. Soc. Rev.* **2022**, *51*, 4094–4120.
- (17) (a) Xu, S.; Zhang, Y.; Li, B.; Liu, S.-Y. Site- and Stereo-selective trans-Hydroboration of 1,3-Enynes Catalyzed by 1,4-Azaborine-Based Phosphine-Pd Complex. J. Am. Chem. Soc. 2016, 138, 14566—14569. (b) Zhang, Y.; Li, B.; Liu, S.-Y. Pd-Senphos Catalyzed trans-Selective Cyanoboration of 1,3-Enynes. Angew. Chem., Int. Ed. 2020, 59, 15928—15932. (c) Wang, Z.; Wu, J.; Lamine, W.; Li, B.; Sotiropoulos, J.-M.; Chrostowska, A.; Miqueu, K.; Liu, S.-Y. C-Boron Enolates Enable Palladium Catalyzed Carboboration of Internal 1,3-Enynes. Angew. Chem., Int. Ed. 2021, 60, 21231—21236.
- (18) (a) Yang, Y.; Jiang, J.; Yu, H.; Shi, J. Mechanism and Origin of the Stereoselectivity in the Palladium-Catalyzed *trans* Hydroboration of Internal 1,3-Enynes with an Azaborine-Based Phosphine Ligand. *Chem. Eur. J.* 2018, 24, 178–186. (b) Zhang, Y.; Wang, Z.; Lamine, W.; Xu, S.; Li, B.; Chrostowska, A.; Miqueu, K.; Liu, S.-Y. Mechanism of Pd/Senphos-Catalyzed *trans*-Hydroboration of 1,3-Enynes: Experimental and Computational Evidence in Support of the Unusual Outer-Sphere Oxidative Addition Pathway. *J. Org. Chem.* 2023, 88, 2415–2424. (c) Wang, Z.; Lamine, W.; Miqueu, K.; Liu, S.-Y. A *syn* outer-sphere oxidative addition: the reaction mechanism in Pd/Senphos-catalyzed carboboration of 1,3-enynes. *Chem. Sci.* 2023, 14, 2082–2090.
- (19) Wang, Z.; Zhang, C.; Wu, J.; Li, B.; Chrostowska, A.; Karamanis, P.; Liu, S.-Y. *trans*-Hydroalkynylation of Internal 1,3-Enynes Enabled by Cooperative Catalysis. *J. Am. Chem. Soc.* **2023**, 145, 5624–5630.
- (20) For cooperative activation of ketones by $B(C_6F_5)_3/NR_3$, see: (a) Chan, J. Z.; Yao, W.; Hastings, B. T.; Lok, C. K.; Wasa, M. Direct Mannich-Type Reactions Promoted by Frustrated Lewis Acid/Brønsted Base Catalysts. *Angew. Chem., Int. Ed.* **2016**, *55*, 13877–13881. (b) Shang, M.; Wang, X.; Koo, S. M.; Youn, J.; Chan, J. Z.; Yao, W.; Hastings, B. T.; Wasa, M. Frustrated Lewis Acid/Brønsted Base Catalysts for Direct Enantioselective α -Amination of Carbonyl Compounds. *J. Am. Chem. Soc.* **2017**, *139*, 95–98. (c) Lam, J.; Szkop, K. M.; Mosaferi, E.; Stephan, D. W. FLP catalysis: main group hydrogenations of organic unsaturated substrates. *Chem. Soc. Rev.* **2019**, *48*, 3592–3612.
- (21) Xu, S.; Haeffner, F.; Li, B.; Zakharov, L. N.; Liu, S.-Y. Monobenzofused 1,4-azaborines: synthesis, characterization, and discovery of a unique coordination mode. *Angew. Chem., Int. Ed.* **2014**, *53*, 6795–6799.
- (22) Reetz, M. T.; Kyung, S. H.; Hüllmann, M. CH3Li/TiCl4: A Non-Basic and Highly Selective Grignard Analogue. *Tetrahedron* **1986**, 42, 2931–2935.

- (23) Zhang, Z.; Liu, C.; Kinder, R. E.; Han, X.; Qian, H.; Widenhoefer, R. A. Highly Active Au(I) Catalyst for the Intramolecular Exo-Hydrofunctionalization of Allenes with Carbon, Nitrogen, and Oxygen Nucleophiles. *J. Am. Chem. Soc.* **2006**, 128, 9066–9073.
- (24) Yang, Y.; Perry, I. B.; Lu, G.; Liu, P.; Buchwald, S. L. Copper-Catalyzed Asymmetric Addition of Olefin-Derived Nucleophiles to Ketones. *Science* **2016**, 353, 144–150.
- (25) Meng, F.; Jang, H.; Jung, B.; Hoveyda, A. H. Cu-Catalyzed Chemoselective Preparation of 2-(Pinacolato)Boron-Substituted Allylcopper Complexes and Their In Situ Site-, Diastereo-, and Enantioselective Additions to Aldehydes and Ketones. *Angew. Chem., Int. Ed.* 2013, 52, 5046–5051.
- (26) Parks, D. J.; Piers, W. E.; Parvez, M.; Atencio, R.; Zaworotko, M. J. Synthesis and solution and solid-state structures of tris-(pentafluorophenyl)borane adducts of PhC(O)X (X = H, Me, OEt, Ni-Pr₂). Organometallics **1998**, *17*, 1369–1377.
- (27) Blackwell, J. M.; Piers, W. E.; McDonald, R. Mechanistic Studies on the $B(C_6F_5)_3$ Catalyzed Allylstannation of Aromatic Aldehydes with Ortho Donor Substituents. *J. Am. Chem. Soc.* **2002**, 124, 1295–1306.
- (28) Blackmond, D. G. Reaction Progress Kinetic Analysis: A Powerful Methodology for Mechanistic Studies of Complex Catalytic Reactions. *Angew. Chem., Int. Ed.* **2005**, *44*, 4302–4320.
- (29) For stoichiometric protonation of unsaturated hydrocarbons coordinated to low-valent metals, see: (a) Casey, C. P.; Chung, S.; Ha, Y.; Powell, D. R. Formation of platinum allyl and propargyl complexes from protonation of platinum enyne and diyne complexes. *Inorg. Chim. Acta* 1997, 265, 127–138. (b) Casey, C. P.; Chung, S. Protonation of rhenium 1,3-enyne and 1,3-diyne complexes: formation of exo-alkylidene eta-3-allyl and eta-3-propargyl complexes. *Inorg. Chim. Acta* 2002, 334, 283–293.
- (30) For catalytic examples of palladium-bound diyne protonation, see: (a) Camacho, D. H.; Saito, S.; Yamamoto, Y. 'Anti-Wacker'-type hydroalkoxylation of diynes catalyzed by palladium(0). *Tetrahedron Lett.* **2002**, 43, 1085–1088. (b) Liu, J.; Schneider, C.; Yang, J.; Wei, Z.; Jiao, H.; Franke, R.; Jackstell, R.; Beller, M. A General and Highly Selective Palladium-Catalyzed Hydroamidation of 1,3-Diynes. *Angew. Chem., Int. Ed.* **2021**, 60, 371–379.
- (31) Because the equilibrium favors the ammonium boron enolate species, the concentration of [1a-NH] can then be approximated as being equal to the concentration of the limiting catalyst.
- (32) Marenich, A. V.; Cramer, C. J.; Truhlar, D. G. Universal Solvation Model Based on Solute Electron Density and on a Continuum Model of the Solvent Defined by the Bulk Dielectric Constant and Atomic Surface Tensions. *J. Phys. Chem. B* **2009**, *113*, 6378–6396.
- (33) Chai, J.-D.; Head-Gordon, M. Long-range Corrected Hybrid Density Functionals with Damped Atom—atom Dispersion Corrections. *Phys. Chem. Chem. Phys.* **2008**, *10*, 6615—6620.
- (34) (a) Andrae, D.; Häussermann, U.; Dolg, M.; Stoll, H.; Preuss, H. Energy-adjusted ab-initio Pseudopotentials for the Second and Third Row Transition Elements. *Theor. Chim. Acta.* **1990**, *77*, 123–141. (b) Dolg, M. *Modern Methods and Algorithm of Quantum Chemistry*; Grotendorst, J.; John von Neuman Institute for Computing: Jülich, Germany, 2000; Vol. 1, pp 479–501. (c) Ehlers, A. W.; Böhme, M.; Dapprich, S.; Gobbi, A.; Höllwarth, A.; Jonas, V.; Köhler, K. F.; Stegmann, R.; Veldkamp, A.; Frenking, G. A set of f-polarization Functions for Pseudo-potential Basis Sets of the Transition Metals Sc-Cu, Y-Ag and La-Au. *Chem. Phys. Lett.* **1993**, 208, 111–114.
- (35) Tamke, S.; Qu, Z. W.; Sitte, N. A.; Florke, U.; Grimme, S.; Paradies, J. Frustrated Lewis Pair-Catalyzed Cycloisomerization of 1,5-Enynes via a 5-endo-dig Cyclization/Protodeborylation Sequence. *Angew. Chem., Int. Ed.* **2016**, *55*, 4336–4339.
- (36) Park, S.; Malcolmson, S. J. Development and Mechanistic Investigations of Enantioselective Pd-Catalyzed Intermolecular Hydroaminations of Internal Dienes. ACS Catal. 2018, 8, 8468–8476.